

REDUCING OF TORQUE AND FLUX RIPPLES IN DTC OF IM BASED ON PREDICTIVE CONTROL

L. DJAGHDALI, S. BELKACEM, F. NACERI

E-mail: djaghdali1@yahoo.fr, belkacem_sebti@yahoo.fr, nacerifarid@yahoo.fr

Department of electrical engineering university of Batna , Algeria

Abstract: We present in this paper a comparative study between two control strategies of electrical machines: Direct Torque Control (DTC-SVM), and Predictive Direct Torque Control (MPDTC). The first algorithm based on PI controllers, where the torque and the flux are regulated by a PI controller; we present a conception method of the PI controllers, associated with the flux and the torque regulation loops and gives analytical formulas for the proportional and integral gains. We also present in the second algorithm. The Predictive Direct Torque Control based on the linearization input-output of the machine. The technique of the linearization is used to give a model linearized and uncoupled from the machine for the anticipation of future behavior of the output. Following the formulation of both approaches, their implementation in the Matlab-Simulink environment has been treated. It has been found that the second approach MPDTC yields high dynamic performances in the whole speed range. These performances are characterized by a low torque ripple. However, requires much more CPU time than the first one.

Key words: Induction motor, direct torque control, Predictive direct torque control, space vector modulation (SVM).

1. INTRODUCTION

The constantly increasing need for better industrial drives (fastest dynamic response, parameter robustness, algorithm simplicity, among others) has encouraged researchers to develop new control strategies to comply with these requirements. New alternatives to both linear and nonlinear methods have been proposed using predictive algorithms to achieve high-bandwidth control loops [1]. The main difficulty in the asynchronous machine control resides in the fact that complex coupling exists between the field and the torque, the direct torque control ensures decoupling between these variables.

Direct Torque Control (DTC) was introduced in the mid 1980's by Takahashi [2]. As a new approach for

torque and flux control of the Induction Machine (IM). The basic idea of DTC is to control the torque and flux linkage by selecting one of the voltage vectors generated by a VSI in order to maintain flux and torque within the limits of two hysteresis bands. The right selection of the vector voltages allows a decoupled control of flux and torque, without the d-q coordinate transformation, PWM and PI current regulators that Field Oriented Control (FOC) needs.

DTC offers advantages such as lower parameter dependency and complexity compared with the FOC, which makes the system more robust and easier to implement. There have been some DTC-based strategies, e.g, voltage-vector selection using switching table direct self-control [3], and space-vector modulation.

Among them, the voltage vector selection strategy using a switching table (usually referred to as DTC) is widely researched and commercialized because it is very simple in concept and easy to be implemented without complicated over modulation technique, which is unavoidable in space vector pulse width modulation (PWM) [5].

However, some research is still being done to adapt DTC to new motors and converters and also to reduce the drawbacks that have been stated in the literature. Among them are the variable switching frequency, which varies according to the motor speed and the hysteresis bands of torque and flux [6], and the high control sampling time (below 25 μ s) that is required to achieve good performance [7].

However, the major DTC system drawback is its relatively high torque ripple. Basically, the high current and torque ripple in DTC are due to the presence of hysteresis comparators together the limited number of available voltage vectors [6]. Since the introduction of the DTC, research has been done to solve these problems, and specially the torque ripple [8].

Reduction of the ripple torque could be obtained by calculation of the stator flux vector variation required to exactly compensate the flux and torque errors. Moreover, the control system should be able to generate any voltage vector, which implies the use of Space Vector Pulse Modulation (SVPWM) [4, 5], and complicates the control scheme.

Another alternative to increase the number of available vectors is an on-line modulation between active and null vectors, in order to obtain a theoretically infinite number of applicable vectors in each of the six spatial directions originated by the power inverter. Although this technique can reduce the torque and flux ripples, more than six vectors directions are necessary to achieve a decoupled control of flux and torque of the machine. For example, in [9, 10] the simple switching table is replaced by several switching tables, obtaining a combination of three voltage vectors into the same sampling period.

We present in this paper a comparative study between two control strategies of electrical machines. The first approach is a control algorithm DTC-SVM, based on PI controllers. The algorithm retains the basic idea of the technique DTC [2] [3]. For this, the technique of orientation of the stator flux is used. Thus, the control voltages can be generated by PI and imposed by SVM technique [18]. This control structure has the advantages of vector control and direct torque control and helps overcome the problems of conventional DTC [11]. PI and vector modulation technique is used to obtain a fixed switching frequency. The second approach. The Predictive Direct Torque Control based on the linearization input-output of induction machine, this control is a technique of advanced control automation [12]. It aims to control complex industrial systems [13]. The principle of this technique is to use a dynamic model of the process inside the controller in real time to anticipate the future behavior of the process [12,14]. It is to be optimized, based on inputs/outputs of a system, predicting the future behavior of the system under consideration. The prediction is made from an internal model of the system on a finite interval of time called the prediction horizon [15]. This control strategy has shown its efficiency, flexibility and success in industrial applications, even for systems with low sampling period [23].

Within these approaches, the paper devotes to a comparative study between the performances of two DTC-SVM: The comparison is based on several criteria including: static and dynamic performance, structure and implementation complexity, decoupling, torque and stator flux ripple.

This paper is organized in seven sections. The model of the induction machine is presented in the next section. The control method by DTC-SVM and MPDTC will be

discussed in section three and four. In the fifth and sixth sections, we present the technique of Space Vector Pulse Width Modulation (SVM) and we compare the simulation results. Finally, a general conclusion summarizes this work. The simulation results are obtained by using Matlab/Simulink.

2. MODEL OF THE INDUCTION MACHINE.

Among the various types of models used to represent the induction machine, there is one that uses each of the stator currents, stator flux, and speed as state variables, voltages (V_{sd} , V_{sq}) as control variables. This model is presented in reference (d, q), related to the rotating field. This model is expressed by the following system of equations [21] [22]:

$$\begin{cases} V_{ds} = R_s \cdot I_{ds} + \frac{d\Phi_{ds}}{dt} - \omega_s \cdot \Phi_{qs} \\ V_{qs} = R_s \cdot I_{qs} + \frac{d\Phi_{qs}}{dt} + \omega_s \cdot \Phi_{ds} \\ V_{dr} = 0 = R_r \cdot I_{dr} + \frac{d\Phi_{dr}}{dt} - (\omega_s - p\Omega) \cdot \Phi_{qr} \\ V_{qr} = 0 = R_r \cdot I_{qr} + \frac{d\Phi_{qr}}{dt} + (\omega_s - p\Omega) \cdot \Phi_{dr} \end{cases} \quad (1)$$

In addition, the components of the stator and rotor flux are expressed by:

$$\begin{cases} \Phi_{ds} = L_s \cdot I_{ds} + L_m \cdot I_{dr} \\ \Phi_{qs} = L_s \cdot I_{qs} + L_m \cdot I_{qr} \\ \Phi_{dr} = L_r \cdot I_{dr} + L_m \cdot I_{ds} \\ \Phi_{qr} = L_r \cdot I_{qr} + L_m \cdot I_{qs} \end{cases} \quad (2)$$

Moreover, the mechanical equation of the machine is given by :

$$J \frac{d\Omega}{dt} + f\Omega = T_e - T_r \quad (3)$$

The electromagnetic torque equation can be expressed in terms of stator currents and stator flux as follows:

$$T_e = P \cdot (\Phi_{ds} \cdot I_{qs} - \Phi_{qs} \cdot I_{ds}) \quad (4)$$

3. DIRECT TORQUE CONTROL (DTC-SVM)

In this control we present a method of analytical design of the PI controllers associated with the control loops of the flux and torque; thereby give analytical formulas for the proportional and integral parameters of the regulator, according to the parameters of the machine.

The block diagram of the control structure is shown in (Fig. 1). Two PI controllers are used for controlling the flux and torque, and another for the speed regulation.

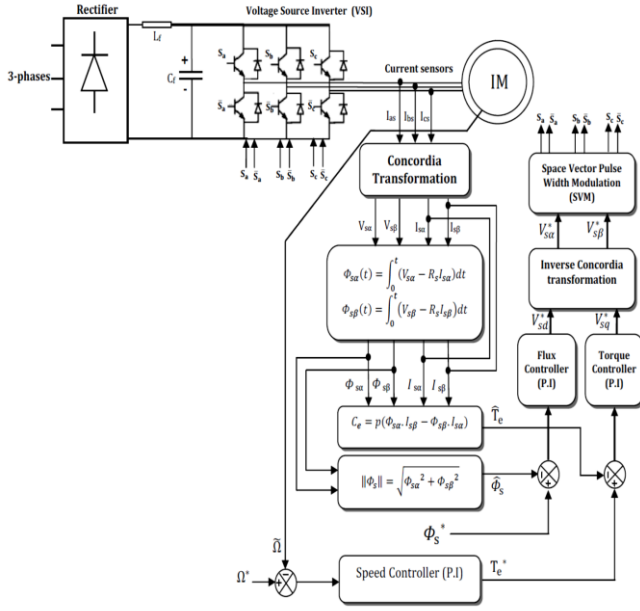


Fig. 1 Diagram of DTC-SVM control of induction machine based on PI controllers.

3.1 Control of the stator flux

In the case of the stator flux orientation in the repository (d, q) (Fig. 2), the axis 'd' coincides with the direction of the stator flux vector $\vec{\Phi}_s$. The 'd' axis component of the stator current I_{sd} is then directly proportional to the magnitude of the stator flux. By controlling and maintaining constant the amplitude of the component of the stator current I_{sd} , we obtain the decoupling of the torque control and the flux of the machine.

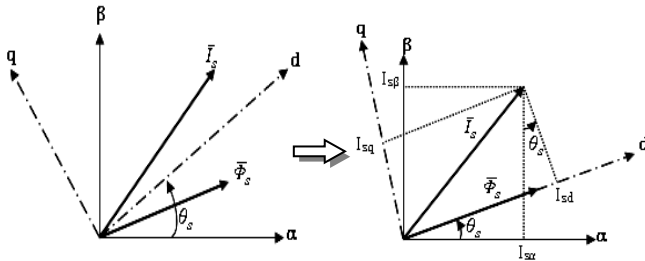


Fig. 2 Vectorial representation of the strategy orientation of stator flux

From the machine model developed previously, we can deduce an expression of stator flux vector. So if the stator flux is oriented on the axis we find:

$$\Phi_{sd} = \Phi_s \text{ and } \Phi_{sq} = 0 \quad (5)$$

Then (1) guesses:

$$\begin{cases} V_{ds} = R_s \cdot I_{ds} + \frac{d\Phi_s}{dt} \\ V_{qs} = R_s \cdot I_{qs} + \omega_s \cdot \Phi_s \\ V_{dr} = 0 = R_r \cdot I_{dr} + \frac{d\Phi_{dr}}{dt} - (\omega_s - p\Omega) \cdot \Phi_{qr} \\ V_{qr} = 0 = R_r \cdot I_{qr} + \frac{d\Phi_{qr}}{dt} + (\omega_s - p\Omega) \cdot \Phi_{dr} \end{cases} \quad (6)$$

The torque becomes:

$$T_e = P \cdot \Phi_s \cdot I_{qs} \quad (7)$$

Autopilot with the law:

$$\omega_s = \omega_r + p\Omega \quad (8)$$

Currents and rotor flux can be expressed as a function of the stator currents by:

$$\begin{cases} I_{dr} = \frac{1}{L_m} (\Phi_s - L_s I_{ds}) \\ I_{qr} = -\frac{L_s}{L_m} I_{qs} \end{cases} \quad (9)$$

$$\begin{cases} \Phi_{dr} = \frac{L_r}{L_m} (\Phi_s - \sigma L_s I_{ds}) \\ \Phi_{qr} = -\frac{\sigma L_s L_r}{L_m} I_{qs} \end{cases} \quad (10)$$

By substituting (9), (10) in (6), and taking, into account the Laplace transform, we get:

$$\Phi_s = \left((1 + \sigma t_r s) I_{ds} + \sigma t_r I_{qs} w_r \right) \frac{L_s}{1 + \sigma t_r s} \quad (11)$$

$$I_{qs} = \left(\frac{1}{L_s} \Phi_s - \sigma I_{ds} \right) \frac{t_r w_r}{1 + \sigma t_r s} \quad (12)$$

With: $t_r = \frac{L_r}{R_r}$, $t_s = \frac{L_s}{R_s}$: the constants time respectively rotor, stator, σ : its leakage coefficient. Expressing the 'd' component of the stator current as a function of the 'q' component of the stator flux and the stator voltages are expressed as follows:

$$\begin{cases} V_{ds} = \frac{\Phi_s}{G_{\Phi_s}} + E_d \\ V_{qs} \approx \omega_s \cdot \Phi_s \end{cases} \quad (13)$$

With:

$$G_{\Phi_s} = \frac{t_s(1 + \sigma t_r s)}{1 + (t_r + t_s)s + \sigma t_r t_s s^2} \quad (14)$$

$$E_d = -\frac{\sigma R_s t_r}{1 + \sigma t_r s} I_{qs} w_r \quad (15)$$

Thus the stator flux can be controlled by the d-component of the stator voltage. (Fig. 3) shows the relationship between Φ_s and V_{ds} , an equivalent system with a second-order perturbation E_d . [18].

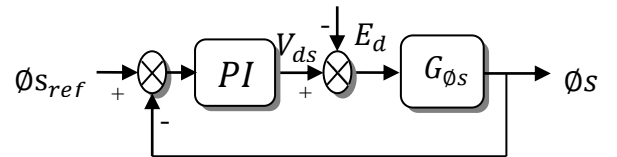


Fig. 3 Block diagram of the flux control

3.2 Calculating Parameters of the PI Regulator of the Flux:

The transfer function of the PI is given by:

$$\begin{aligned} C(s) &= K_{pf} + \frac{K_{if}}{s} = K_{pf} \left(1 + \frac{1}{\tau_f s} \right) \\ &= K_{pf} \frac{(1 + \tau_f s)}{\tau_f s} \end{aligned} \quad (16)$$

Where K_{pf} , K_{if} denote proportional and integral gains of the corrector, and

$\tau_f = \frac{K_{pf}}{K_{if}}$: Is time constant.

The transfer function of the open loop (TFOL) is given by:

$$\begin{aligned} TFOL &= C(s) \cdot G_{\phi_s} \\ &= K_{pf} \frac{(1 + \tau_f s)}{\tau_f s} \cdot \frac{t_s(1 + \sigma t_r s)}{1 + (t_r + t_s)s + \sigma t_r t_s s^2} \end{aligned} \quad (17)$$

From the command "roots" in Matlab, one can find the roots of the polynomial:

$$1 + (t_r + t_s)s + \sigma t_r t_s s^2$$

There are two roots:

$$P_1 = f(t_r, t_s, \sigma)$$

$$P_2 = f(t_r, t_s, \sigma)$$

So, we removed the pole dominating, which is the pole nearest to the imaginary axis (either the pole P_2).

We can rewrite the relation (17) in form pole-zero as follows:

$$TFOL = K_{pf} \frac{\left(\frac{1}{\tau_f} + s \right)}{s} \cdot \frac{\sigma t_r t_s \left(\frac{1}{\sigma t_r} + s \right)}{(s - P_1)(s - P_2)} \quad (18)$$

To eliminate the dominant pole:

$$(s - P_2) = \left(\frac{1}{\tau_f} + s \right) \quad (19)$$

We get:

$$TFOL = \frac{K_{pf}}{s} \cdot \frac{t_s(1 + \sigma t_r s)}{(s - P_1)} \quad (20)$$

The transfer function in closed loop (TFCL) is written as follows:

$$TFCL = \frac{TFOL}{1 + TFOL} \quad (21)$$

By substituting (20) into (21) and after simplification we get:

$$TFCL = \frac{K_{pf} t_s (1 + \sigma t_r s)}{s^2 + (K_{pf} t_s \sigma t_r - P_1)s + K_{pf} t_s} \quad (22)$$

To control the closed loop system, it is necessary to choose the coefficients K_{pf} and K_{if} . For this, we use the method of the imposition of the poles.

The transfer function of a standard second order system is characterized by:

$$F(s) = \frac{k \omega_n^2}{s^2 + 2\xi \omega_n s + \omega_n^2} \quad (23)$$

Where ξ and ω_n are the damping coefficient and the natural angular frequency of the system.

By analogy between the expressions (22) and (23) taking into account the expression (19), we find:

$$\begin{cases} (s - P_2) = \left(s + \frac{1}{\tau_f} \right) \\ 2\xi \omega_n = (K_{pf} t_s \sigma t_r - P_1) \\ \left\{ \begin{array}{l} \frac{1}{\tau_f} = -P_2 \Rightarrow K_{if} = -K_{pf} P_2 \\ K_{pf} = \frac{2\xi \omega_n + P_1}{t_s \sigma t_r} \end{array} \right. \end{cases} \quad (24)$$

Gains which are obtained for the corrector have a minimum response time while ensuring the absence of overshoot. This technique involves the imposition of values damping and the pulsation to determine the coefficients K_{pf} and K_{if} .

3.3 Control of the electromagnetic torque

From relations (11), (12), the current along the axis 'q' can be expressed as:

$$I_{qs} = \frac{t_r(1 - \sigma)}{L_s} \frac{\Phi_s w_r}{(1 + \sigma t_r s)^2 + (\sigma t_r w_r s)^2} \quad (25)$$

Substituting (25) into (7) gives:

$$T_e = p \frac{t_r(1 - \sigma)}{L_s} \frac{\Phi_s^2 w_r}{(1 + \sigma t_r s)^2 + (\sigma t_r w_r s)^2} \quad (26)$$

As the modulus of the vector $\overline{\Phi_s}$ remains constant and equal to its reference value Φ_s^* , and $\sigma t_r \ll 1$, the relationship (26) can be simplified as follows [18]:

$$T_e = p \frac{t_r(1 - \sigma)}{L_s} \frac{\Phi_s^{*2}}{(1 + 2\sigma t_r s)} (\omega_s - p\Omega) \quad (27)$$

The electromagnetic torque is proportional to the slip pulse, so equation (27) can be written as follows:

$$T_e = G_{T_e} (\omega_s - p\Omega) \quad (28)$$

Where

$$G_{T_e} = p \frac{t_r(1 - \sigma)}{L_s} \frac{\Phi_s^{*2}}{(1 + 2\sigma t_r s)} \quad (29)$$

The torque can be controlled by the stator pulsation. (Fig. 4) shows the relationship between T_e and ω_s . A PI controller is used to achieve the desired performance and maintain the torque reference value $T_{e \text{ ref}}$.

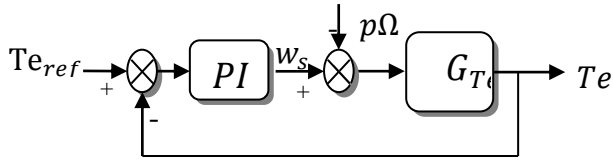


Fig. 4 Block diagram of torque control.

3.4 Calculating parameters of the PI regulator of the torque:

The transfer function of the PI is given by:

$$\begin{aligned} C(s) &= K_{pc} + \frac{K_{ic}}{s} \\ &= K_{pc} \left(1 + \frac{1}{\tau_c s} \right) \\ &= K_{pc} \frac{(1 + \tau_c s)}{\tau_c s} \end{aligned} \quad (30)$$

Where K_{pc} , K_{ic} denote proportional and integral gains of the corrector, and

$\tau_c = \frac{K_{pc}}{K_{ic}}$: Is time constant.

The transfer function in a closed loop (TFCL) is given as follows:

$$TFCL = \frac{C(s).G_{Te}}{1 + C(s).G_{Te}} \quad (31)$$

By substituting (29) and (30) into (31), and, after simplification, one finds:

$$\begin{aligned} TFCL &= \frac{K_{ic} P t_r (1 - \sigma) \Phi_s^2 (1 + \tau_c s)}{2 \sigma t_r L_s s^2 + (K_{ic} \tau_c P t_r (1 - \sigma) \Phi_s^2 + L_s) s + K_{ic} P t_r (1 - \sigma) \Phi_s^2} \\ &= \frac{(1 + \tau_c s)}{\frac{2 \sigma t_r L_s}{K_{ic} P t_r (1 - \sigma) \Phi_s^2} s^2 + \frac{(K_{ic} \tau_c P t_r (1 - \sigma) \Phi_s^2 + L_s)}{K_{ic} P t_r (1 - \sigma) \Phi_s^2} s + 1} \end{aligned} \quad (32)$$

TFCL the form of a second order system is characterized by:

$$F(s) = \frac{k}{\frac{1}{\omega_n^2} s^2 + \frac{2\xi}{\omega_n} s + 1} \quad (33)$$

After identification by the equations (32) and (33), we will have:

$$\begin{cases} \frac{1}{\omega_n^2} = \frac{2 \sigma t_r L_s}{K_{ic} P t_r (1 - \sigma) \Phi_s^2} \\ \frac{2\xi}{\omega_n} = \frac{(K_{ic} \tau_c P t_r (1 - \sigma) \Phi_s^2 + L_s)}{K_{ic} P t_r (1 - \sigma) \Phi_s^2} \end{cases} \Rightarrow \begin{cases} K_{ic} = \frac{2 \sigma t_r L_s \omega_n^2}{P t_r (1 - \sigma) \Phi_s^2} \\ \tau_c = \frac{K_{pc}}{K_{ic}} = \frac{2\xi}{\omega_n^2} - \frac{L_s}{K_{ic} P t_r (1 - \sigma) \Phi_s^2} \end{cases} \quad (34)$$

The technique is about imposition of the values pulsation ω_n and damping ξ to determine the coefficients. K_{pc} , K_{ic} .

4. PREDICTIVE DIRECT TORQUE CONTROL (MPDTC)

The Predictive control is a technique of advanced control automation. It aims to control complex industrial systems. The basic principle of predictive control is taken into account, at the current time, the future behavior, through explicit use of a numerical model of the system in order to predict the output in the future, on a finite horizon. One of the advantages of predictive methods lies in the fact that for a pre-calculated set on a horizon, it is possible to exploit the information of predefined trajectories located in the future, given that the aim is to match the output of system with this set on a finite horizon. (Fig. 5)

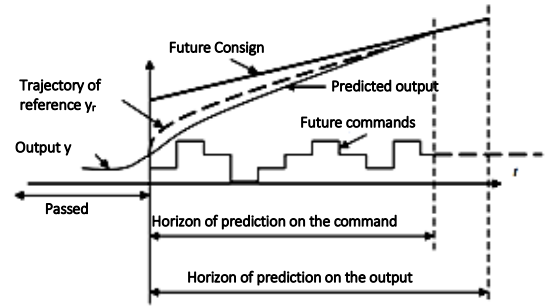


Fig.5 Time Evolution of the Finite Horizon Prediction

4.1 Formulation of The Model

All algorithms predictive control differs from each other by the model used to represent the process and the cost function to be minimized [19]. The process model can take different representations (transfer function, state variables, impulse response...), we will give for our formulation, the technique of the linearization input-output of the induction machine, in order to give a linearized model; module of the stator flux and the torque are uncoupled. The interest of such approach is to linearize the nonlinear model of the machine and to obtain a homogeneous behavior whatever the point of operation.

We recall the system of the equations of the induction machine in the reference (α, β) which is given by:

$$\begin{cases} \frac{dI_{s\alpha}}{dt} = -\left(\frac{R_s}{\sigma L_s} + \frac{R_r}{\sigma L_r}\right) I_{s\alpha} - \omega_r I_{s\beta} + \frac{R_r}{\sigma L_r L_s} \phi_{s\alpha} + \frac{\omega_r}{\sigma L_s} \phi_{s\beta} + \frac{1}{\sigma L_s} V_{s\alpha} \\ \frac{dI_{s\beta}}{dt} = -\left(\frac{R_s}{\sigma L_s} + \frac{R_r}{\sigma L_r}\right) I_{s\beta} + \omega_r I_{s\alpha} + \frac{R_r}{\sigma L_r L_s} \phi_{s\beta} - \frac{\omega_r}{\sigma L_s} \phi_{s\alpha} + \frac{1}{\sigma L_s} V_{s\beta} \\ \frac{d\phi_{s\alpha}}{dt} = V_{s\alpha} - R_s I_{s\alpha} \\ \frac{d\phi_{s\beta}}{dt} = V_{s\beta} - R_s I_{s\beta} \end{cases} \quad \dots (35)$$

The generated torque can be expressed in terms of currents stator and stator flux as follows:

$$T_e = p(\phi_{s\alpha} I_{s\beta} - \phi_{s\beta} I_{s\alpha}) \quad (36)$$

The system of equations receives in the form suggested for the application of the linearization within the meaning of the input-output as follows:

$$\begin{cases} \dot{x} = f(x) + g_1(x)V_{s\alpha} + g_2(x)V_{s\beta} \\ y = h(x) \end{cases} \quad (37)$$

With:

$$f(x) = \begin{bmatrix} f_1(x) \\ f_2(x) \\ f_3(x) \\ f_4(x) \end{bmatrix} = \begin{bmatrix} -\left(\frac{R_s}{\sigma L_s} + \frac{R_r}{\sigma L_r}\right) I_{s\alpha} - \omega_r I_{s\beta} + \frac{R_r}{\sigma L_r L_s} \phi_{s\alpha} + \frac{\omega_r}{\sigma L_s} \phi_{s\beta} \\ -\left(\frac{R_s}{\sigma L_s} + \frac{R_r}{\sigma L_r}\right) I_{s\beta} + \omega_r I_{s\alpha} + \frac{R_r}{\sigma L_r L_s} \phi_{s\beta} - \frac{\omega_r}{\sigma L_s} \phi_{s\alpha} \\ -R_s I_{s\alpha} \\ -R_s I_{s\beta} \end{bmatrix} \quad \dots (38)$$

Where the vector of states x and the commands u are:

$$x = [I_{s\alpha}, I_{s\beta}, \phi_{s\alpha}, \phi_{s\beta}]^t, \quad u = [V_{s\alpha}, V_{s\beta}]^t$$

$$\text{and : } g_1(x) = \left[\frac{1}{\sigma L_s}, 0, 1, 0 \right]^t, g_2(x) = \left[0, \frac{1}{\sigma L_s}, 0, 1 \right]^t$$

4.2.1 Control Flux-Torque:

Our concern is to minimize the pulsations on the level of the torque and the flux of the induction machine. For that, we chose the torque and the module of stator flux like variables to be controlled; thus the vector of output is given by the equation according to:

$$y = \begin{bmatrix} h_1 \\ h_2 \end{bmatrix} = \begin{bmatrix} T_e \\ |\phi_s|^2 \end{bmatrix} = \begin{bmatrix} p(\phi_{s\alpha} I_{s\beta} - \phi_{s\beta} I_{s\alpha}) \\ \phi_{s\alpha}^2 + \phi_{s\beta}^2 \end{bmatrix} \quad (39)$$

4.2.2 Input-Output Linearization:

The method of the input-output linearization is developed starting from the theories of the differential geometry [20]. It consists of using the derivative of Dregs to express the model of the machine in relation to input-output. To obtain the non-linear law of control, let us derive as much from time than it is necessary in order to reveal the entry u . The derivatives of the two outputs are given by:

$$\begin{aligned} \dot{y}_1 &= L_f h_1(x) + L_{g1} h_1(x) V_{s\alpha} + L_{g2} h_1(x) V_{s\beta} \\ &= \sum_{i=1}^4 \frac{\partial h_1}{\partial x_i} f_i(x) + \sum_{i=1}^4 \frac{\partial h_1}{\partial x_i} g_{1i}(x) V_{s\alpha} + \sum_{i=1}^4 \frac{\partial h_1}{\partial x_i} g_{2i}(x) V_{s\beta} \\ \dots (40) \end{aligned}$$

With:

$$\begin{aligned} L_f h_1 &= -p\phi_{s\beta} \left[-\left(\frac{R_s}{\sigma L_s} + \frac{R_r}{\sigma L_r}\right) I_{s\alpha} - \omega_r I_{s\beta} + \frac{R_r}{\sigma L_r L_s} \phi_{s\alpha} + \frac{\omega_r}{\sigma L_s} \phi_{s\beta} \right] \\ &\quad + p\phi_{s\alpha} \left[-\left(\frac{R_s}{\sigma L_s} + \frac{R_r}{\sigma L_r}\right) I_{s\beta} + \omega_r I_{s\alpha} + \frac{R_r}{\sigma L_r L_s} \phi_{s\beta} - \frac{\omega_r}{\sigma L_s} \phi_{s\alpha} \right] \\ L_{g1} h_1 &= p(I_{s\beta} - \frac{1}{\sigma L_s} \phi_{s\beta}) \end{aligned}$$

$$L_{g2} h_1 = p(\frac{1}{\sigma L_s} \phi_{s\alpha} - I_{s\alpha}) \quad (41)$$

$$\begin{aligned} \dot{y}_2 &= L_f h_2(x) + L_{g1} h_2(x) V_{s\alpha} + L_{g2} h_2(x) V_{s\beta} \\ &= \sum_{i=1}^4 \frac{\partial h_2}{\partial x_i} f_i(x) + \sum_{i=1}^4 \frac{\partial h_2}{\partial x_i} g_{1i}(x) V_{s\alpha} + \sum_{i=1}^4 \frac{\partial h_2}{\partial x_i} g_{2i}(x) V_{s\beta} \dots (42) \end{aligned}$$

With:

$$\begin{cases} L_f h_2 = -2R_s(\phi_{s\alpha} I_{s\alpha} - \phi_{s\beta} I_{s\beta}) \\ L_{g1} h_2 = 2\phi_{s\alpha} \\ L_{g2} h_2 = 2\phi_{s\beta} \end{cases} \quad (43)$$

4.2.3 Linearization of the System:

The matrix defining the relation between the inputs of the system and its derived outputs is given by the expression:

$$\begin{bmatrix} \dot{y}_1 \\ \dot{y}_2 \end{bmatrix} = A(x) + D(x) \begin{bmatrix} V_{s\alpha} \\ V_{s\beta} \end{bmatrix} \quad (44)$$

With:

$$\begin{aligned} A(x) &= \begin{bmatrix} L_f h_1 \\ L_f h_2 \end{bmatrix}; \\ D(x) &= \begin{bmatrix} L_{g1} h_1 & L_{g2} h_1 \\ L_{g1} h_2 & L_{g2} h_2 \end{bmatrix} = \begin{bmatrix} p(I_{s\beta} - \frac{1}{\sigma L_s} \phi_{s\beta}) & p(\frac{1}{\sigma L_s} \phi_{s\alpha} - I_{s\alpha}) \\ 2\phi_{s\alpha} & 2\phi_{s\beta} \end{bmatrix} \end{aligned}$$

$D(x)$: Matrix of decoupling.

$$\text{Det } [D(x)] = p \left(I_{s\beta} - \frac{1}{\sigma L_s} \phi_{s\beta} \right) \cdot 2\phi_{s\beta} - p \left(\frac{1}{\sigma L_s} \phi_{s\alpha} - I_{s\alpha} \right) \cdot 2\phi_{s\alpha} \dots (45)$$

After simplification, we get:

$$\text{det}[D(x)] = 2p \left[\frac{-1}{\sigma L_s} (\phi_{s\beta}^2 + \phi_{s\alpha}^2) + I_{s\beta} \phi_{s\beta} + I_{s\alpha} \phi_{s\alpha} \right] \neq 0 \dots (46)$$

The determinant of the matrix $D(x)$ is different from zero; therefore $D(x)$ is an invertible matrix.

$$\begin{aligned} D^{-1}(x) &= \frac{1}{2p \left[\frac{-1}{\sigma L_s} (\phi_{s\beta}^2 + \phi_{s\alpha}^2) + I_{s\beta} \phi_{s\beta} + I_{s\alpha} \phi_{s\alpha} \right]} \begin{bmatrix} 2\phi_{s\beta} & -p(\frac{1}{\sigma L_s} \phi_{s\alpha} - I_{s\alpha}) \\ -2\phi_{s\alpha} & p(I_{s\beta} - \frac{1}{\sigma L_s} \phi_{s\beta}) \end{bmatrix} \quad (47) \end{aligned}$$

The linearization following input-output which is introduced for the system illustrated by (eq-37) is given by:

$$\begin{bmatrix} V_{s\alpha} \\ V_{s\beta} \end{bmatrix} = D^{-1}(x) \left[-A(x) + \begin{bmatrix} V_1 \\ V_2 \end{bmatrix} \right] \quad (48)$$

$V = \begin{bmatrix} V_1 \\ V_2 \end{bmatrix}$: represent the new vector of input.

The application of the law linearizing (48) on the system

(44) led to two linear and uncoupled mono variable systems:

$$\begin{cases} V_1 = \dot{h}_1(x) \\ V_2 = \dot{h}_2(x) \end{cases} \quad (49)$$

To ensure perfect regulation and track the desired signals of the flux and torque toward their reference, V_1 and V_2 are chosen as follows.

$$\begin{cases} V_1 = |\dot{\phi}_s|_{\text{ref}}^2 + k_1(|\phi_s|_{\text{ref}}^2 - |\phi_s|^2) \\ V_2 = \dot{T}_{e \text{ ref}} + k_2(T_{e \text{ ref}} - T_e) \end{cases} \quad (50)$$

Here, the subscript 'ref' denotes the reference value and (k_1, k_2) are constant design parameters to be determined in order to make the decoupled system in (44) stable. The behavior of the linearized model is imposed by the pole placement method. The coefficients selected, such as $s + k_1$ and $s + k_2$, are the Hurwitz polynomials [16,17].

4.2. Criterion of Optimization

We must find the future control sequence to apply on the system to reach the desired set point by following the reference trajectory. To do this, we just minimize a cost function which differs according to the methods, but generally this function contains the squared errors between the reference trajectory and the predictions of the prediction horizon and the variation of the control [14]. This cost function is given as follows:

$$J = \sum_{j=N_1}^{N_2} [w(t+j) - \hat{y}(t+j)]^2 + \lambda \sum_{j=1}^{N_u} \Delta u(t+j-1)^2$$

... (51)

With:

$w(t+j)$: Set point applied at time $(t+j)$.

$\hat{y}(t+j)$: Output predicted time $(t+j)$. $\Delta u(t+j-1)$:

Increment of control at the moment $(t+j-1)$.

N_1 : Minimum prediction horizon on the output.

N_2 : Maximum prediction horizon on the output, with $N_2 \geq N_1$.

N_u : Horizon prediction on the order.

λ : Weighting factor on the order.

T_s : The period of sampling.

4.3 Choice of the Parameters of Control

The definition of the quadratic criterion (equa-51) showed that the user must set four parameters. The choice of parameters is difficult because there is no empirical relationship to relate these parameters to conventional

measures automatically.

N_1 : minimum horizon of prediction is the pure delay system if the delay is known; or we should initialize to 1.

N_2 : maximum horizon is chosen so that the product $N_2 T_s$ is limited by the value of the desired response time. Indeed increase beyond the prediction of the response time provides no additional information].

N_u : horizon of control, we should choose equal to 1 and not exceeding the value of two [24].

λ : weighting factor of the control, this is the most complicated to set parameter since it influences the stability of the closed loop system [24]. Indeed, if λ is very high, it helps to balance the influence of the orders in the optimization.

The model is linearized and uncoupled from the induction machine, so that it is established inside the predictive control, which is shown by (Fig. 6).

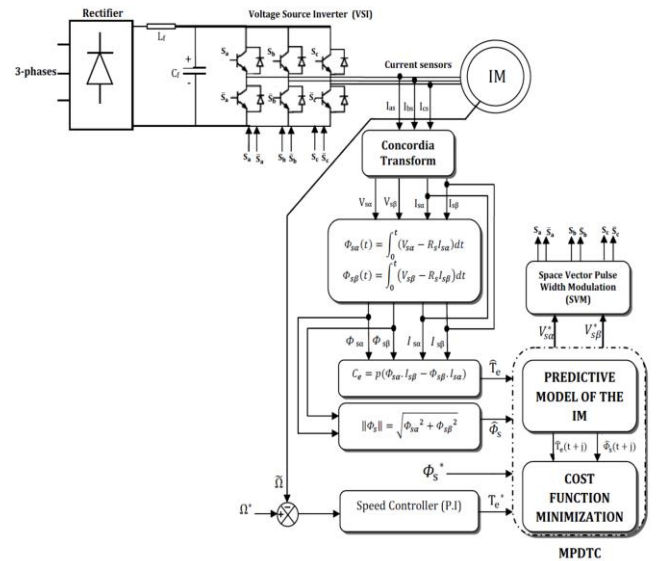


Fig. 6 Diagram block of the predictive direct torque control

5. SPACE VECTOR PULSE WIDTH MODULATION

The SVM technique refers to a special switching scheme of the six power transistors of a 3-phase PWM inverter. In fact, The SVM technique uses eight sorts of different switch modes of inverter to control the stator flux to approach the reference flux circle. It attains the higher control performances. Eight sorts of switch modes are corresponding respectively to eight space voltage vectors that contain six active voltage vectors and two zero voltage vectors. The six active voltage vectors form the axes of a hexagon. The two zero voltage vectors are at the origin [25]. The eight vectors are called the basic space vectors. E.g. V_1 (100), $S_a = 1$ denotes the upper leg of a phase is switched on, $S_b = 0$ and $S_c = 0$ mean the lower legs of b and c phases is off. The voltage vectors, produced by a 3-phase PWM inverter, divide the space vector plane into six Sectors as shown in (Fig. 7).

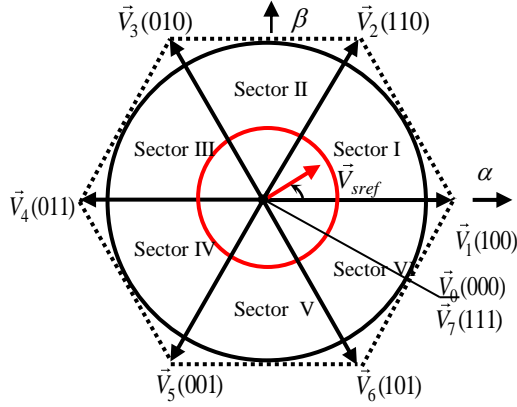


Fig. 7 Switching States of Space Vector Modulation.

In every sector, the voltage vector is arbitrary synthesized by basic space voltage vector of the two sides of one sector and zero vectors [16]. For example, in the first sector (Fig. 8), \bar{V}_{sref} is a synthesized voltage, space vector and its equation is given by:

$$\bar{V}_{sref} T_s = \bar{V}_0 T_0 + \bar{V}_1 T_1 + \bar{V}_2 T_2 \quad (52)$$

$$T_s = T_0 + T_1 + T_2 \quad (53)$$

Where, T_0 , T_1 and T_2 is the work time of basic space voltage vectors \bar{V}_0 , \bar{V}_1 and \bar{V}_2 respectively.

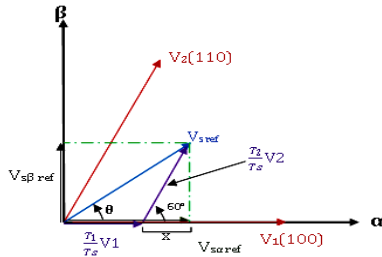


Fig. 8 Projection of the Reference Voltage Vector

The determination of the Amount of times T_1 and T_2 given by mere projections is:

$$\begin{cases} V_{s\alpha ref} = \frac{T_1}{T_s} |\bar{V}_1| + x & T_1 = \frac{T_s}{2U_{dc}} (\sqrt{6}V_{s\alpha ref} - \sqrt{2}V_{s\beta ref}) \\ V_{s\beta ref} = \frac{T_2}{T_s} |\bar{V}_2| \sin(\frac{\pi}{3}) \Rightarrow T_2 = \frac{T_s \sqrt{2}}{U_{dc}} V_{s\beta ref} \\ x = \frac{V_{s\beta ref}}{\tan(\frac{\pi}{3})} \end{cases} \quad \dots (54)$$

The rest of the period is applying the null-vector. For every sector, switching duration is calculated. The amount of times of the vector implementation can all be related to the following variables:

$$\begin{cases} X = \frac{T_s}{U_{dc}} (\sqrt{2}V_{s\beta ref}) \\ Y = \frac{T_s}{2U_{dc}} (\sqrt{6}V_{s\alpha ref} + \sqrt{2}V_{s\beta ref}) \\ Z = \frac{T_s}{2U_{dc}} (-\sqrt{6}V_{s\alpha ref} + \sqrt{2}V_{s\beta ref}) \end{cases} \quad (55)$$

The implementation of the duration's sector boundary vectors is tabulated as follows:

Table. I Durations of the Sector Boundary Vectors

SECTOR	1	2	3	4	5	6
T_1	-Z	Y	X	Z	-Y	-X
T_{I+1}	X	Z	-Y	-X	-Z	Y

The third step is to compute the duty cycles that have three necessary times:

$$\begin{cases} T_{aon} = \frac{T_s - T_i - T_{i+1}}{2} \\ T_{bon} = T_{aon} + T_i \\ T_{con} = T_{bon} + T_{i+1} \end{cases} \quad (56)$$

The last step is to assign the right duty cycle (T_{xon}) to the right motor phase according to the sector.

Table. II Assigned Duty Cycles to the PWM Outputs

Sector	1	2	3	4	5	6
S_a	T_{aon}	T_{bon}	T_{con}	T_{con}	T_{bon}	T_{aon}
S_b	T_{bon}	T_{aon}	T_{aon}	T_{bon}	T_{con}	T_{con}
S_c	T_{con}	T_{con}	T_{bon}	T_{aon}	T_{aon}	T_{bon}

6. THE RESULTS OF SIMULATIONS

a. Electromagnetic Torque

It is found that the predictive direct torque control has a high dynamic performance of the electromagnetic torque acting very quickly by following the instructions load introduced. The latter has a remarkable decrease in the amplitude of the oscillations from the DTC-SVM.

b. The Speed of Rotation

It is found that the speed reaches its reference $\Omega_{ref} = 100 \text{rd/s}$ without overshoot and releases disturbance due to load instructions applied to various aforementioned moments are almost eliminated. MPDTC control this release very fast perturbation of the DTC-SVM.

c. The stator flux

The module of the stator flux is quickly established at its reference value 1.11Wb in both control techniques. The MPDTC has a visible reduction in oscillation amplitude and the modulus of the flux with respect to the DTC-SVM.

The dynamic component of the stator flux is not affected by the application of the load command, but has unwanted circulations at startup in MPDTC.

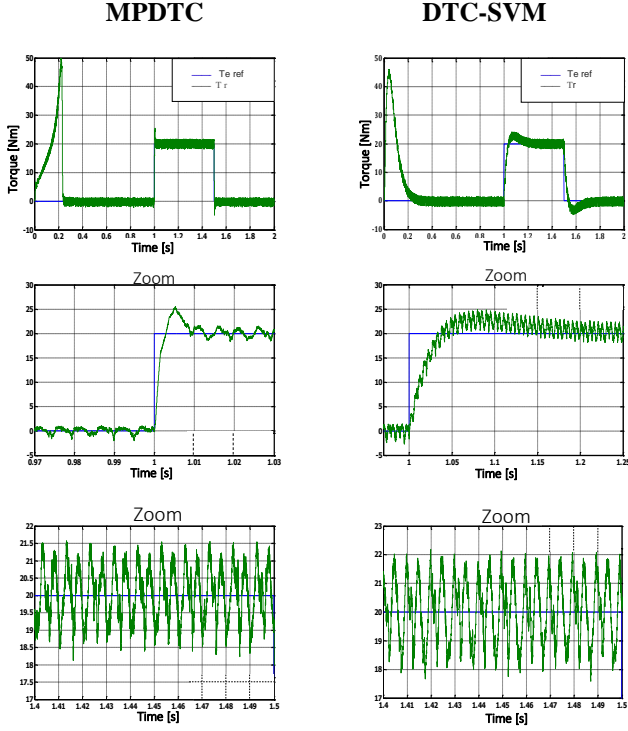


Fig.9 Comparison of the electromagnetic torque

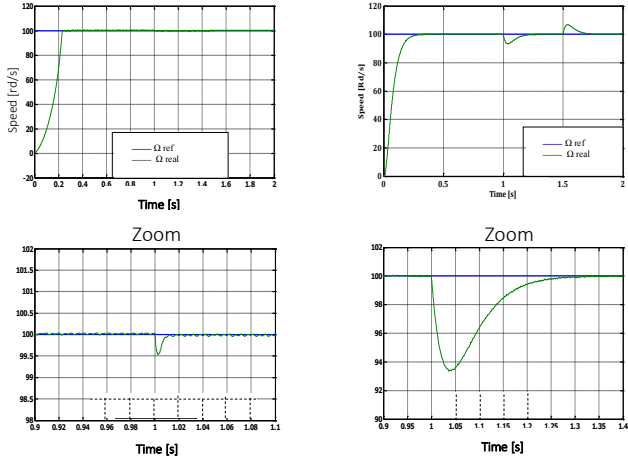


Fig . 10 Comparison of the speed of rotation

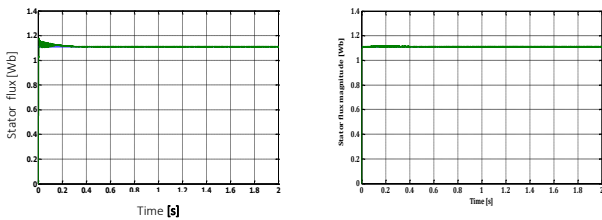


Fig.11 Comparison of The stator flux

Table III summarizes the results of the comparative study treated previously. In fact, from table III, one can choose the approach to be used according to the needed objectives, the desired performances and the available means.

Table III. Comparison between Performances of the two DTC-SVM Approaches

Control Approach	DTC-SVM	MPDTC
Commutation frequency	fixed	fixed
Electromagnetic torque ripples	high	low
Stator flux ripples	high	low
Switching losses	high	low
rejection of disturbance	Bad	good
Algorithm complexity	low	high
computing time	low	high

7. CONCLUSION

In this paper, the principle and several characteristics of Direct Torque Control and Predictive Direct Torque Control schemes for Induction Motor drive, are studied by simulation in order to determinate the main advantages and drawbacks of each control, and to make a comparison between them.

The simulation results show that the MPDTC control provides better dynamic performance in torque and stator flux module, as well as rejection disturbance. The stator current is sinusoidal (less harmonics), comparing with the DTC-SVM.

However, the toughness can be improved by increasing the weighting factor by acting on the adjustment parameters of the predictive controller. These parameters have a decisive influence on the system behavior. But it is not always easy to find optimal values for these parameters.

CHARACTERISTICS OF THE MACHINE USED FOR SIMULATION:

parameter	symbol	Value
Number of pole pairs	p	2
Power	P _u	3 KW
Line voltage	U _n	380V
Line current	I _n	6.3A
Nominal frequency	f	50Hz
Mechanical rotor speed	N _n	1430 tr/mn
Electromagnetic torque	T _e	20Nm
Stator Resistance	R _s	3.36 Ω
Rotor Resistance	R _r	1.09 Ω
Stator cyclic inductance	L _s	0.256H
Mutual cyclic Inductance	L _m	0.236H
Rotor cyclic inductance	L _r	0.256H
Rotor inertia	j	4,5.10 ⁻² Kg. m2
Viscosity coefficient	f	6,32.10 ⁻⁴ N.m.sec.

8. References.

- [1] H. Miranda, P.Cortés, Juan I. Yuz, and J.Rodriguez. "Predictive Torque Control of Induction Machines Based on State-Space Models". *IEEE Trans. Ind. Electron.*, VOL. 56, NO. 6, JUNE 2009.
- [2] I. Takahashi, Y. Ohmori. "High-Performance Direct Torque Control of an Motor". *IEEE Trans. on Industrial Applications*, 25(2):257–264, March/April 1989.
- [3] M. Depenbrock. "Direct Self-Control (DSC) of Inverter-Fed Induction Machine". *IEEE Trans. on Power Electronics*, 3(4):420–429, October 1988.
- [4] S. Babu, S. Ushakumari "Modified Direct Torque Control of Induction Motor Drives" Recent Advances in Intelligent Computational Systems (RAICS), 2011 IEEE, Pages: 937 – 940.
- [5] W. Xie, X. Wang, G. Dajaku, D. Gerling, R. Kennel. "Improvement and Comparison of Efficiency and Low Cost Drive System based on DTC and DTC-SVM". *Electric Machines & Drives Conference (IEMDC)*, 2013 IEEE International, Pages: 1261 – 1266.
- [6] K. Shyu; J. Lin, V. Pham, M. Yang, T. Wang. "Global Minimum Torque Ripple Design for Direct Torque Control of Induction Motor Drives". *Industrial Electronics, IEEE Transactions*, Year: 2010, Volume: 57, Issue: 9, Pages: 3148 – 3156.
- [7] Kumar. T.V, Rao. S.S. "Direct torque control method for induction motor drives based on modified amplitude and angle decoupled control of stator flux". *Power Electronics, Drives and Energy Systems (PEDES) & 2010 Power India*, 2010 Joint International Conference, Year: 2010. Pages: 1 – 6.
- [8] G. S. Buja, and M. P. Kazmierkowski, "Direct Torque Control of PWM Inverter-Fed AC Motors—A Survey", *IEEE Trans. on Ind. Electronics*, .vol.51, no. 4, pp. 744-757, August 2002.
- [9] Sarika, E.P.; Praveen Raj, R.S. "Performance comparison of direct torque control of two level and three level neutral point clamped inverter fed three phase induction motor". *Advances in Green Energy (ICAGE)*, 2014 International Conference, Year: 2014, Pages: 179 - 183,
- [10] M. HABIBULLAH, D.D.-C. Lu. "Model predictive duty based torque and flux ripples minimization of induction motor drive". *Power Electronics, Machines and Drives (PEMD 2014)*, 7th IET International Conference Year: 2014, Pages: 1 – 6.
- [11] H. Hiba, H. Ali, H. Othmen. "DTC-SVM control for three phase induction motors". *Electrical Engineering and Software Applications (ICEESA)*, 2013 International Conference. Year: 2013, Pages: 1 – 7.
- [12] G. Papafotiou, J. Kley, K. G. Papadopoulos, P. Bohren, and M. Morari. "Model predictive direct torque control - part II: Implementation and experimental evaluation". *IEEE Trans. Ind. Electron.*, 56(6):1906–1915, Jun. 2009.
- [13] L. Wei; S. Mei. "Direct torque control of induction machines based on predictive control" *Control Conference (CCC)*, 2010 29th Chinese. Year: 2010, Pages: 3295 – 3300.
- [14] T.Geyer. "Generalized Model Predictive Direct Torque Control: Long Prediction Horizons and Minimization of Switching Losses". *Joint 48th IEEE Conference on Decision and Control and 28th Chinese Control Conference Shanghai, P.R. China*, December 16-18, 2009.
- [15] P. Cortès, M. P. Kazmierkowski, R. M. Kennel, D. E. Quevedo, and J. Rodriguez. "Predictive Control in Power Electronics and Drives". *IEEE transactions on industrial electronics*. 55(12):4312–4324, Dec. 2008.
- [16] S. Belkacem, F. Naceri, R. Abdessemed, "Robust nonlinear control for direct torque control of induction motor drive using space vector modulation", *Journal of Electrical Engineering*, Vol. 10, pp. 79-87, 2010.
- [17] Decoupling control of induction motors based on nonlinear optimal predictive control Chuanfu Jin; Yanguang Sun; Qinghai Fang *Control and Automation (ICCA)*, 2010 8th IEEE International Conference Year: 2010, Pages: 1048 – 1052.
- [18] M. Bounadja, A.W.Belarbi, B.Belmadani "A high performance svm-dtc scheme for induction machines have integrated starter generator in hybrid electric vehicles". *Journal Nature and Technology*. No. 02 / January 2010. pages 41 to 47.
- [19] E.F. Camacho, C.Bordons, "Model Predictive Control", Springer-Verlag London, 2^{ème} édition, 2003.
- [20] C. JIN, Y. SUN, Q.FANG "Decoupling Control of Induction Motors based on Nonlinear Optimal Predictive Control". *Control and Automation (ICCA)*, 2010 8th IEEE International Conference Year: 2010, Pages: 1048 – 1052.
- [21] C. Carlsson of Wit "Modeling and Vector Control DTC". *Science Edition Hermes Europe*, 2000.
- [22] G. Grellet, G. Clerc, "Electric Actuators, Principle, Models, Order". *Electro Collection*. Eyrolles Edition 2000.
- [23] T. Geyer. G. Papafotiou, M. Fellow "Model predictive Direct Torque Control-Part I: Concept, Algorithm, and Analysis". *IEEE transactions on industrial electronics*, Vol.56, No.6 JUNE 2009; pp1894-1905.
- [24] J. B. Rawlings and D. Q. Mayne. "Model predictive control: Theory and design". *Nob Hill Publ* 2009.